# Multi-Agent Persistent Monitoring via Time-Inverted Kuramoto Dynamics

Manuel Boldrer, Fabio Pasqualetti, Luigi Palopoli, Daniele Fontanelli

***Abstract*— We present a novel distributed multi-robot coordination strategy to persistently monitor a closed path-like environment. Our monitoring strategy relies on a class of time-inverted Kuramoto dynamics, whose multiple equilibria coincide with different monitoring configurations and allow us to tune the covering time of specific areas based on their priority. We provide a detailed analysis of the equilibria of the considered class of time-inverted Kuramoto dynamics and demonstrate the effectiveness of the proposed monitoring strategy via numerical examples.**

***Index Terms*— Time-inverted Kuramoto dynamics, persistent monitoring, multiagent systems, nonlinear networked systems.**

## I. Introduction

Distributed control algorithms for the coordination of teams of robots have received increasing attention in the last years. In this area, one fundamental problem is to deploy robots to persistently and dynamically patrol, or monitor, an area of interest, which finds application for service and maintenance, event detection, and surveillance, among others. In this paper we propose and analyze a novel distributed strategy for the persistent monitoring of one-dimensional closed regions.

### A. Related work

In the last decade several researchers have studied the problem of persistent monitoring. In [15] the authors formally introduce the idea of persistent monitoring in a changing environment and present a linear program formulation. The problem of monitoring a set of stationary points of interest is studied in [14]. In [11], given different priorities to different points of interest, the authors propose a method to generate the route through graph-theoretic techniques, and then to coordinate the robots to obtain equal-time-spacing trajectories. Kingston et al. [7] present a decentralized algorithm for perimeter surveillance; the algorithm manages changing perimeters and insertion/deletion of agents. In [1] a non-deterministic patrolling algorithm is considered to deal with an adversarial setting. A solution for dynamic perimeter surveillance is presented in [13], [6]. An optimal persistent monitoring problem is formulated in [4] in a one-dimensional space and in a two-dimensional space in [10]. Soltero et al. [16] account for the collision avoidance in persistent monitoring problem on intersecting trajectories. Finally, [12] proposes a perimeter surveillance strategy based on artificial vector fields for three-dimensional mission spaces.

M. Boldrer and D. Fontanelli are with the Deparment of Industrial Engineering, University of Trento, Italy {manuel.boldrer, daniele.fontanelli}@unitn.it

L. Palopoli are with the Department of Information Engineering and Computer Science, University of Trento, Italy luigi.palopoli@unitn.it

F. Pasqualetti is with Department of Mechanical Engineering at the University of California, Riverside, fabiopas@engr.ucr.edu

Differently from the existing literature, in this paper we propose a novel strategy for single-agents and clustered persistent monitoring of a one-dimensional closed path, where multiple agents repeatedly visit all points of the path in different coordinated fashion. The case of single-agents monitoring proves useful when the monitoring objective is, for instance, to detect deterministic events, while the clustered case is particularly appropriate when multiple measurements at the same location increase the detection probability, and it also improves the reliability of the monitoring strategy against agent failures.

### B. Paper contribution and organization

We propose a novel distributed monitoring strategy based on a class of time-inverted Kuramoto dynamics. The proposed strategy allows us to tune the monitoring priority of different locations in a one-dimensional closed environment, and to dynamically modify them through sparse control actions. Our strategy is based on the translation of the desired monitoring task into the property of the equilibria of the considered class of time-inverted Kuramoto dynamics, which we can characterize and control by operating on the parametric description of the curve that describes the trajectory of the robots. Finally, we provide a set of numerical experiments to validate the effectiveness of the proposed strategy.

A preliminary version of the results contained in this paper was presented in [2]. However, compared to [2] we made several advances: we provide Theorem 1, which in the previous version was **informally addressed**. In addition, this paper shows Theorem 2, which was presented in [2] just as a conjecture. The core of the novel contribution are the results that link persistent monitoring (Section III) with the properties of the Kuramoto equilibria. Finally, we offer here a rich numeric validation of our results.

The paper is organized as follows. Section II describes our problem setup and presents the analysis of the time-inverted Kuramoto dynamics. Section III contains our persistent monitoring strategy. Finally, Section IV presents our numerical results and Section V concludes the paper.

## II. Problem setup and preliminary results

The persistent monitoring problem that we are going to address in this paper is the following: given a closed path $\mathcal{P} \subset \mathbb{R}^3$ and $N$ robotic agents, steer the robots in a configuration such that each point $q \in \mathcal{P}$ is periodically visited by one or multiple robots, with a constant frequency.

### A. Connectivity and motion constraints

*1) Multi-agent network:* The interconnection between the $N$ robots are described by the undirected graph $\mathcal{G}(\mathcal{V}, \mathcal{E})$, where

$\mathcal{V} = \{1, \dots, n\}$ denotes the set of robots and $\mathcal{E} \subseteq \mathcal{V} \times \mathcal{V}$ their interconnections. Let us indicate with $\mathcal{V}(i)$ the $i$–th entry of the set $\mathcal{V}$. In this work we focus on ring-like interconnections, where $\mathcal{E} = \{(\mathcal{V}(i), j) \ : \ j = \mathcal{V}(i+1)\} \cup \{(\mathcal{V}(i), j) \ : \ j = \mathcal{V}(i-1)\}\} \cup \{(\mathcal{V}(1), \mathcal{V}(N))\} \cup \{(\mathcal{V}(N), \mathcal{V}(1))\}$ and the order of the $\mathcal{V}$ entries is arbitrary (i.e., it is not necessarily a 2-circulant topology). In the rest of the paper we refer to the ring topology edge set as $\mathcal{R}$, and let $\mathcal{R}_i = \{j \ : \ (i,j) \in \mathcal{R}\}$.

*2) Motion constraints:* We assume that the robots are constrained to move on the closed path $\mathcal{P} \subset \mathbb{R}^3$, which can be written in parametric form as $r(\gamma) : \mathbb{R} \to \mathbb{R}^3$. The state of the $i$–th robot is $\theta_i \in \mathbb{R}$, while its position on $\mathcal{P}$ is $r(\theta_i)$. **We assume that it is possible to directly control the $i$–th state velocity $\dot{\theta}_i, \forall i$.** For clarity, in Fig. 1, the path of interest $\mathcal{P}$ is a circle (dashed blue line), where $r(\gamma) = [\cos\gamma, \sin\gamma, 0]$ and the robots' positions $r(\theta) = [r(\theta_1), r(\theta_2), \dots, r(\theta_N)]^\top$ are depicted with blue filled circles.

### B. Robot dynamics

We let the state of each robot evolve according to a class of time-inverted Kuramoto dynamics. In particular,

$$\dot{\theta}_i = \omega - \sum_{j \in \mathcal{R}_i} \sin\left(\theta_j - \theta_i\right), \ \ \forall i = 1, \dots, N, \tag{1}$$

where $\omega$ is the natural frequency parameter. Compared to the classic homogeneous Kuramoto model [8], where all agents typically converge to a phase-synchronized state, the negative sign in (1) and the fixed ring topology force the robots to converge to different, stable, splay-state configurations, as we discuss next. **In the following we will implicitly observe the evolution of the angles from a mobile reference frame that rotates with constant speed $\omega$. Hence, by assuming that all the agents have the same natural frequency $\omega$, we can consider $\omega = 0$ without loss of generality.**

**Theorem 1** (Convergence to the equilibrium)**. The dynamical system (1) converges to an equilibrium point**

$$\begin{aligned}\theta^{\star(p)} = [\theta_0 + 2z_1\pi, \theta_0 + 2z_2\pi + \frac{2\pi p}{N}, \dots \\ \dots, \theta_0 + 2z_N\pi + \frac{2\pi p(N-1)}{N}]^\top,\end{aligned} \tag{2}$$

*where $\theta_0 \in \mathbb{R}$ can be any real number, $p \in \{(N/4 + kN, 3N/4 + kN) \cap \mathbb{Z}\}$, and $z_i, k \in \mathbb{Z}$ for all $i = 1 \dots N$.*

*Proof.* Firstly, we prove that the system converges to an equilibrium point. The undirected graph $\mathcal{G}(\mathcal{V}, \mathcal{R})$, which has $\text{card}(\mathcal{V}) = N$ number of nodes and $\text{card}(\mathcal{R}) = M = N$ number of edges, can be uniquely associated with a directed graph obtained introducing a direction to the arc according to the lexographical order of the nodes it connects (i.e., if $e = \{i, j\} \in \mathcal{R}$ with $i < j$ then the orientation of the arc in the directed graph will be from $i$ to $j$). Define $B \in \mathbb{R}^{N \times M}$ as the incidence matrix of the directed graph just introduced. The dynamics can be written in the more compact form: $\dot{\theta} = B \sin(B^\top \theta)$, where $\theta = [\theta_1, \theta_2, \cdots, \theta_N]^\top$ and where we consider the sin function as applied element-wise to vector $B^\top\theta$. By selecting as a Lyapunov function

$$V(\theta) = \frac{N^2 - 2N + 2\,\mathbf{1}_N^\top \cos\left(B^\top\theta\right)}{N^2}, \tag{3}$$

**with the gradient with respect to $\theta$ being $\nabla_\theta V = -\frac{2}{N^2} B \sin\left(B^\top\theta\right)$, the time derivative of (3) is equal to**

$$\dot{V}(\theta) = \nabla_\theta V^\top \dot{\theta} = -\frac{2}{N^2}\dot{\theta}^\top\dot{\theta} \leq 0,$$

by the LaSalle invariance principle [9] the system converges to an equilibrium point.

Directly from the dynamics (1), it follows that the necessary condition for the equilibrium is $\sum_{j \in \mathcal{R}_i} \sin\left(\theta_i - \theta_j\right) = 0, \forall i = 1, \dots, N$. Hence, all the possible equilibrium points have to belong to the symmetric set $\theta^{\star(p)}$ (2), where $p \in \mathbb{Z}$, or to the set $\theta^\star_{(z)} = [\theta_0 + z_1\pi, \theta_0 + z_2\pi, \dots, \theta_0 + z_N\pi]^\top$, where $\sin(\theta_i - \theta_j) = 0, \ \ \forall j \in \mathcal{R}_i$ and $\forall i = 1 \dots N$.

By computing the Jacobian $A$ **around the candidate equilibrium points, we obtain**

$$A = \begin{cases} a_{ii} = \sum_{j \in \mathcal{R}_i} \cos\left(\theta_j^\star - \theta_i^\star\right) \\ a_{hi} = \begin{cases} -\cos\left(\theta_h^\star - \theta_i^\star\right), & h \in \mathcal{R}_i \\ 0, & h \notin \mathcal{R}_i. \end{cases} \end{cases} \tag{4}$$

**From the Jacobian matrix (4), it turns out that, if the condition $\sum_{j \in \mathcal{R}_i} \cos(\theta_j^\star - \theta_i^\star) > 0$ is true for at least one agent, the equilibrium is unstable. Moreover, since for at least one agent the condition $\sum_{j \in \mathcal{R}_i} \cos(\theta_j^\star - \theta_i^\star) < 0$ has to be satisfied, we can discard the equilibria $\theta^\star_{(z)}$. In fact, the only configuration in $\theta^\star_{(z)}$, which leads to a candidate stable equilibrium, it is contained in $\theta^{\star(p)}$ (i.e. $\theta^{\star(N/2)}$ ), hence we can focus only on the equilibrium configurations in (2). By exploiting the properties of circulant matrices [5], we can express the eigenvalues of $A$ in closed form:**

$$\lambda_r(A) = -2\cos\left(\frac{2\pi p}{N}\right)\left[-1 + \cos\left(\frac{2\pi r}{N}\right)\right].$$

**Since $\cos\left(\frac{2\pi p}{N}\right) = \cos(\theta_i^{\star(p)} - \theta_j^{\star(p)})$, it follows that necessary condition for stability is given by $\cos(\theta_i^{\star(p)} - \theta_j^{\star(p)}) < 0, \ \ \forall j \in \mathcal{R}_i$ and $\forall i = 1 \dots N$.** Thus, the equilibria in (2) are stable if and only if $p \in \{(N/4 + kN, 3N/4 + kN) \cap \mathbb{Z}\}$, where $k \in \mathbb{Z}$. By choosing $p \in \{(N/4 + kN, 3N/4 + kN) \cap \mathbb{Z}\}$, the linearized dynamics has a single eigenvalue equal to zero because of the $\theta_0$ rotations; all the others eigenvalues are negative. □

**In this work we refer to splay-state configuration as the equilibria in (2).** In Fig. 1 we depict some examples for the possible equilibrium configurations with different number of agents. **Notice that we depict only the set $p \in \{0, \lfloor N/2 \rfloor] \cap \mathbb{Z}\}$, since $p \in \{\lceil N/2 \rceil, N) \cap \mathbb{Z}\}$ contains equivalent equilibrium configurations, e.g., let us consider $N = 7$, the equilibrium configurations with $p = \{0, 1, 2, 3\}$ are equivalent to the equilibrium configurations with $p = \{7, 6, 5, 4\}$ respectively, we will use this fact later in the paper. More formally, we can state the following:**

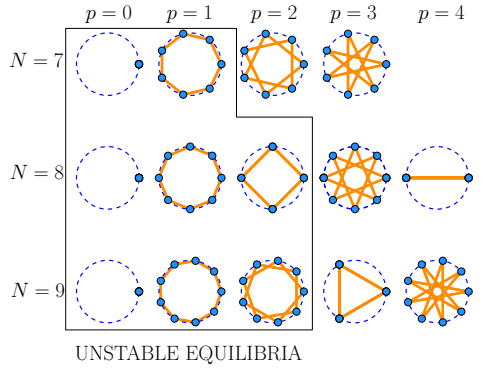


**Fig. 1:** Equilibrium configurations (2), for the dynamical model in (1). We depict the equilibrium configurations by changing the values for $p$ by considering the number of agents $N = 7, 8, 9$. The blue filled circles represent the agents while the orange links indicate the graph topology.

**Remark 1.** **By selecting $p \in \{(0, N) \cap \mathbb{Z}\}$ in equation (2), the equilibrium configurations can be split into two equivalent sets $p_1 \in I_1$ and $p_2 \in I_2$, where $I_1 = \{(0, \lfloor N/2 \rfloor] \cap \mathbb{Z}\}$ and $I_2 = \{[\lceil N/2 \rceil, N) \cap \mathbb{Z}\}$. Indeed, let us select $p_1$ equal to the $i$–th component of the $I_1$ interval, i.e., $p_1 = I_1[i]$, and let us select $p_2 = I_2[N + 1 - i]$, $\forall i = 1 \dots$ card$(I_1)$, by construction of (2), it follows that mod$(\theta_j^{\star(p_1)}, 2\pi) \equiv$ mod$(\theta_{N+2-j}^{\star(p_2)}, 2\pi)$ $\forall j = 2 \dots N$ (by assuming the same $\theta_0$ value).**

The following result is instrumental to our analysis. Firstly, let us define what we meant by cluster:

**Definition 1** (Cluster)**.** *A group $\mathcal{Y}$ of robots forms a cluster if $\theta_i - \theta_j = 2k\pi$, for every $i, j \in \mathcal{Y}$ and some $k \in \mathbb{Z}$.*

**Lemma 1** ($\kappa$-clustered coverage)**.** *Given $N > 2$ and the dynamics* (1)*, the number of agents that clusters together at the stable equilibrium points* (2) *is given by the greater common divisor between $N$ and $p$, denoted by $\kappa = gcd(N, p)$. The clusters divide the circle in $N/\kappa$ equal parts ($\kappa$-clustered coverage).*

*Proof.* See [2] for a proof of this result. □

We conclude this section with a result concerning the controllability properties of the nonlinear system (1). In what follows, we show how different equilibrium configurations can be obtained by simply controlling the position of one robot.[1] Let us call $\mathcal{C}$ the set of controllable agents.

**Theorem 2** (Control of the final equilibrium)**.** *Let $N > 2$. If the agents are in a stable configuration with a value of $p \in \{(N/4, \lfloor N/2 \rfloor) \cap \mathbb{Z}\}$ and the position of a single agent $i \in \mathcal{C}$ is changed from $\theta_i$ to $\theta_i + \pi$, then the system* (1) *converges to the equilibrium configuration corresponding to $p^+ \in \mathbb{Z}$, with $p < p^+ \leq \lceil N/2 \rceil$.*

*Proof.* Without loss of generality, let us consider $\mathcal{C} = \{1\}$. Under the conditions stated above the following statements hold true:

1) Let us consider a 2-circulant topology, i.e. an ordered ring topology, to simplify the notation, then $\dot{\theta}_1 = 0$, $\dot{\theta}_{N-k} \leq 0$, $\dot{\theta}_{2+k} \geq 0$, $\forall t$ and for $k = 0, \dots, \lfloor N/2 \rfloor$.
2) **Let us define $\Delta\theta_{ij}^{\star(p)} = \|$mod$(\theta_i^{\star(p)}, 2\pi) -$ mod$(\theta_j^{\star(p)}, 2\pi)\|$,** then $\Delta\theta_{ij}^{\star(p^+)} > \Delta\theta_{ij}^{\star(p)}$, where $p^+$ is the value of $p$ associated with the configuration reached after the perturbation $\delta\theta_1 = \pi$.

Because of the symmetry of the splay-state solutions $\theta^{\star(p)}$ in (2) and the symmetry of the equilibrium configurations with respect to the perturbation $\delta\theta_1 = \pi$, it follows from the dynamics (1) that $\dot{\theta}_1 = 0$ and $\dot{\theta}_{2+k} = -\dot{\theta}_{N-k}$ for $k = 0, \dots, \lfloor N/2 \rfloor - 1$. If we hypothesize that an agent changes it's velocity in sign during the evolution of the system, all the agents have to do so in a symmetric fashion, since $\dot{\theta}_{2+k} = -\dot{\theta}_{N-k}$ for $k = 0, \dots, \lfloor N/2 \rfloor - 1$. However, since $\dot{V} \leq 0$ (see Theorem 1), this is not possible because it would imply to go back to a configuration with an higher Lyapunov function value. Hence, since the perturbation of agent 1 by $\delta\theta_1 = \pi$, leads to $\dot{\theta}_2 < 0$ and $\dot{\theta}_N > 0$ when $p \in \{(N/4, \lfloor N/2 \rfloor) \cap \mathbb{Z}\}$ ($\dot{\theta}_2 > 0$ and $\dot{\theta}_N < 0$ when $p \in \{(\lceil N/2 \rceil, 3N/4) \cap \mathbb{Z}\}$), by assuming an initial equilibrium configuration $\theta^{\star(p)}$ with $p \in \{(N/4, \lfloor N/2 \rfloor) \cap \mathbb{Z}\}$, the networked dynamics of the system (1) implies $\dot{\theta}_{2+k} \leq 0$, $\dot{\theta}_{N-k} \geq 0$ for $k = 0, \dots, \lfloor N/2 \rfloor - 1$, at any time $t$, hence the statement 1 is satisfied.

By assuming that the system after the perturbation is not in an equilibrium configuration, the statement 1 implies the statement 2, (see Fig. 3 for a clearer visualisation). In fact, according to statement 1, the next reached equilibrium will have a lower value for $\theta_2$ and an higher value for $\theta_N$. Since all the values in between are equidistant mod$(2\pi)$ at the equilibria in (2), the statement 2 is a consequence. Because of Theorem 1, starting from $\theta^{\star(p)}$, by applying the perturbation $\delta\theta_1 = \pi$, the system will converge towards $\theta^{\star(p^+)}$, and since $\Delta\theta_{ij}^{\star(p^+)} > \Delta\theta_{ij}^{\star(p)}$, because of statement 2, the new equilibrium configuration have to satisfy $p^+ > p$. The upper bound $p^+ \leq \lceil N/2 \rceil$, again, comes from the fact that $\dot{V} \leq 0$ (see Theorem 1). Indeed, by considering the Lyapunov function in equation (3) and the equilibrium points (2), it is easy to recognize that $\{\theta^{\star(\lfloor N/2 \rfloor)}, \theta^{\star(\lceil N/2 \rceil)}\} = \arg\min_{\theta \in \theta^{\star(p)}} \mathbf{1}_N^\top \cos\left(B^\top \theta\right)$, with $p \in \{(N/4, 3N/4) \cap \mathbb{Z}\}$, hence the upper bound for $p$ is $\lceil N/2 \rceil$.

□

Fig. 2 shows the evolution of the Lyapunov function $V(\theta)$, by applying four times a perturbation of $\delta\theta_i = \pi$ at different instants of time, while Fig. 3 shows the trajectory of the robot states $\theta$.

## III. Persistent Monitoring Strategy

The persistent monitoring of a generic path of interest $\mathcal{P}$ can be obtained by imposing to the state $\theta_i$ the dynamics in (1) with $\omega > 0$, for each robot in the system. It follows from Theorem 1 that the agents converge to an equilibrium configuration that belongs to (2), which is a $\kappa$-clustered configuration (see Lemma 1). By constraining the $i$–th robot

[1] See https://www.youtube.com/watch?v=AQxW9aP8ugo for an illustrative simulation.

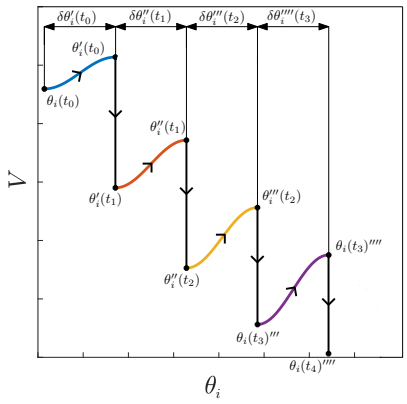


**Fig. 2:** Lyapunov function value evolution in time. At time $t_0$ the system is perturbed from $\theta_i(t_0)$ to $\theta_i'(t_0) = \theta_i(t_0) + \delta\theta'(t_0)$, where $\delta\theta'(t_0) = \pi$. Hence the system reaches the new equilibrium configuration $\theta_i'(t_1)$. This procedure is repeated until it reaches the "most stable" equilibrium configuration.

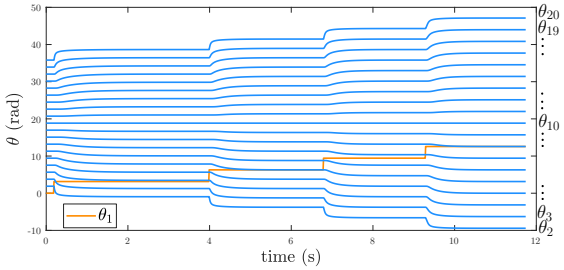


**Fig. 3:** Evolution of the $\theta$ value in time. We are considering the same situation depicted in Fig. 2. It can be notice how the difference $\Delta\theta_{ij}^{\star(p^+)}$ increases after each perturbation.

position to be equal to $r(\theta_i), \forall i = 1 \dots N$, where $r(\gamma) : \mathbb{R} \to \mathbb{R}^3$ is a parametric representation of the path of interest $\mathcal{P}$, the robots will patrol the path in a $\kappa$-clustered configuration. **It means that, at the equilibrium, each point on the path of interest is repeatedly covered by $\kappa = \gcd(N, p)$ robots, with a constant frequency $f = \frac{N/\kappa}{2\pi/\omega}$.** To control the final equilibrium configuration we can rely on Theorem 2, which, however, drives the system towards $p = \lfloor N/2 \rfloor$. In this Section, we provide sufficient conditions to fully control the final equilibrium configuration. Moreover, we show how to take into account different patrolling priorities on different locations on the path of interest.

By acting on the parametric representation $r(\gamma)$ of the path of interest $\mathcal{P}$, we can: i. manipulate the final equilibrium configurations, and ii. assign priorities, in terms of coverage time, to each curve stretch.

Let us start with the equilibrium manipulation. This feature can be very useful in practice, for instance, if the agents have the capability to communicate only with the neighbors in a physical sense, i.e., with the agents in front and behind, or if a clustered persistent monitoring is required. In the presented framework, we are going to show that we can steer the system towards any equilibrium configuration in (2), if the number of agents $N$ is odd, and by controlling the position of a single agent. Let us start by defining a sufficient condition for 1-clustered coverage configuration.

**Theorem 3** (Sufficient condition for 1-clustered coverage configuration)**.** *Given an odd number of agents $N > 2$, by controlling the position of at least 1 agent i.e., card$(\mathcal{C}) \geq 1$, it is always possible to steer the final configuration to the 1-clustered coverage formation.*

*Proof.* Theorem 1 ensures convergence to $\theta^{\star(p)}$ with $p \in \{(N/2, 3N/4) \cap \mathbb{Z}\}$. By using the results of Lemma 1, we know that for $N \in \{2\mathbb{N} + 1\}$, the configurations $\theta^{\star(\lfloor N/2 \rfloor)}$ and $\theta^{\star(\lceil N/2 \rceil)}$ are 1-clustered coverage configurations, since $(N, \frac{(N\pm1)}{2})$ are coprime, i.e., $\gcd(N, \lfloor N/2 \rfloor) = \gcd(N, \lceil N/2 \rceil) = 1$. Moreover, because of Theorem 2, under the assumption that card$(\mathcal{C}) \geq 1$, it is always possible to steer the system towards the equilibrium $\theta^{\star(\lfloor N/2 \rfloor)}$ (or $\theta^{\star(\lceil N/2 \rceil)}$), hence the proof. □

Since we can steer the system to the 1-clustered coverage state, the trick here is to change the parametric representation of the path of interest. In particular, we multiply the parametrization variable by $\alpha \in \mathbb{N}$, obtaining an alternative path $\tilde{r}(\gamma)$. By using this contrivance, we do not change the shape of the path of interest but only its length by a factor $\alpha$, i.e., $\tilde{r}(\gamma)$ has the same shape of $r(\gamma)$, however, by considering $\gamma \in (0, 2\pi)$, it completes multiple laps, repeating the same positions $\alpha$ times. As a consequence, the equilibrium configurations, from the perspective of the "single-lap path" $r(\gamma)$, change in $\tilde{\theta}^{\star(p)} = \alpha\theta^{\star(p)}$.

To recover any $\kappa$-clustered configuration, the greatest common divisor between $N$ and $\alpha$ has to be set equal to $\kappa$, i.e., $\eta = \gcd(N, \alpha) = \kappa$.

More formally we can state the following:

**Lemma 2** (Equilibrium manipulation 1)**.** *Given an odd number of agents $N > 2$, let us consider the following configuration*

$$\theta^{\star(p)} = \left[0, \frac{2\pi p}{N}, \dots, \frac{2\pi p(N-1)}{N}\right]^\top$$

*where $p = \frac{N-1}{2} + kN$, i.e., 1-clustered coverage formation. By considering the alternative configuration $\tilde{\theta}^{\star(p)} = \alpha\theta^{\star(p)}$, let us define $\eta$ as the greatest common divisor between $\alpha$ and $N$, i.e., $\eta = gcd(\alpha, N)$, the resulting alternative configuration is an $\eta$-clustered coverage.*

*Proof.* In this case we obtain the following equilibrium configurations

$$\theta^{\star(p)} = \left[0, \frac{\alpha/\eta\pi(N-1)}{N/\eta}, \dots, \frac{\alpha/\eta\pi(N-1)(N-1)}{N/\eta}\right]^\top.$$

Since $N - 1$ is an even number, $\alpha/\eta$ and $N/\eta$ are integers, it is by construction the $\eta$-clustered configuration. □

Finally, by combining Theorem 3 and Lemma 2 we can conclude that the system, through equilibrium manipulation, can be steered towards any configuration in the set (2), including the unstable configurations.

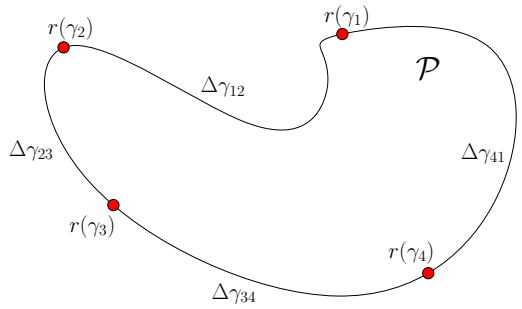


**Fig. 4:** Example of a path of interest $\mathcal{P}$ with 4 points of interest $r(\gamma_i)$.

**Lemma 3** (Equilibrium manipulation 2)**.** *Given an odd number of agents $N > 2$, being in the equilibrium configuration* (2) *with $p = \frac{N-1}{2}$, by considering the modified equilibrium configurations $\tilde{\theta}^{\star(\frac{N-1}{2})} = \alpha\theta^{\star(\frac{N-1}{2})}$, we can reconstruct all the equilibria $\theta^{\star(\bar{p})}$ with $\bar{p} \in \mathbb{N}$, by tuning the parameter $\alpha$.*

*Proof.* Since $\alpha\theta^{\star(\frac{N-1}{2})} = \theta^{\star(\alpha\frac{N-1}{2})}$ and $p = N-1$ is equivalent to $p = 1$ because of Remark 1, by selecting $\alpha = 2\bar{p}$ we have that $\theta^{\star(\bar{p}(N-1))} \equiv \theta^{\star(\bar{p})}$, hence the proof. □

Notice that in Lemma 2 – 3 the number of agents has to be odd, otherwise the configuration $p = \frac{N-1}{2} + kN \notin \mathbb{Z}$ would not be an equilibrium.

**Remark 2.** *We showed that by shaping the path parametrization, we can reach different configurations. However, by manipulating $\alpha$, in particular by increasing it, we have to account for a proportionate increase of the agents' velocities, which is compensated by scaling the natural frequency $\omega$ by the parameter $\alpha$.*

The other feature, that we mentioned before, associated to the path parametrization, is the priority assignement to different locations on the path. Let us consider $z$ points of interest $w = \{w_1, w_2, ..., w_z\}$, where $w_i \in \mathcal{P}$, $\forall i = 1 \dots z$. We can express $\mathcal{P}$ in the parametric form $r(\gamma) = [x(\gamma), y(\gamma), z(\gamma)]^\top$, where $r(\gamma_1) = w_1, r(\gamma_2) = w_2, \dots, r(\gamma_z) = w_z$ . To assign different priorities to different locations on the path, the idea is to modify the parametric representation of the curve $\mathcal{P}$, by scaling $\Delta\gamma_{ij} = \|\gamma_i - \gamma_j\|$ by a factor $f_i$, keeping $\Delta\gamma_{ii} = 2k\pi$.

For the sake of clarity, we depict in Fig. 4 the path $\mathcal{P} \subset \mathbb{R}^2$, the phase differences $\Delta\gamma_{ij}$ and the points of interest $w_i$, where $z = \text{card}(w) = 4$. Let us consider the weighted phase differences $\Delta\tilde{\gamma}_{ij} = f_i\Delta\gamma_{ij}$ , when the priority factor is equal to $f_i = 1\ \forall i$ ($\Delta\tilde{\gamma}_{ij} = \Delta\gamma_{ij}$), the agents' velocities are equal to $v = \sqrt{\dot{x}(\gamma)^2 + \dot{y}(\gamma)^2}$. By imposing $f_1 > 1$ we are proportionally decreasing the agents' speeds at the $l_{12}$ stretch (the agents cover the points on $l_{12}$ for more instants of time), while if $f_1 < 1$, we are proportionally increasing it. In this way we can tune the covering time (i.e., the amount of time spent by the agents in the proximity of the points of interest) to each stretch of the path of interest $\mathcal{P} = \{\mathcal{P}_{12} \cup \mathcal{P}_{23} \cdots \cup \mathcal{P}_{z1}\}$. In the following section we provide some simulation results.

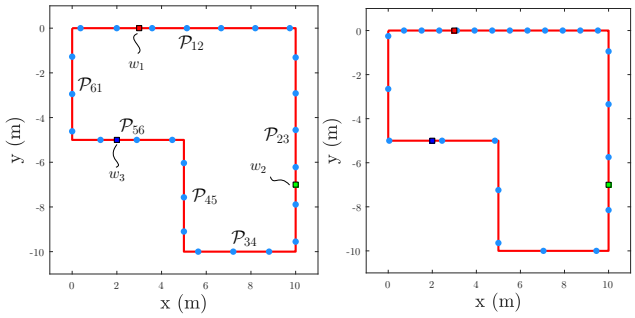


(a) (b)

**Fig. 5:** Simulations with $N = 25$, on a custom path $\mathcal{P}$ with three points of interest depicted with colored squares. (a) No priorities assigned $f_i = f,\ \forall i = 1 \dots 6$ , (b) priorities assigned $f_1 = 3f$, $f_i = f\ \forall i = 2 \dots 6$. Quantitative results on the monitoring time are reported in Table I, in the first (a) and in the second (b) column respectively.

**TABLE I:** Quantitative results of simulation in Fig. 5. Amount of the time spent by the agents in the proximity of the points of interest, by considering a proximity radius of 0.5 m and by changing the priority factors $f_i$.

| - | $f_1 = f_2 = f_5$ | $f_1 = 3f_2 = 3f_5$ | $f_2 = \frac{1}{2}f_1, f_5 = \frac{1}{3}f_1$ | $f_1 = 2f_2, f_5 = 5f_2$ |
|---|---|---|---|---|
| $t_1(s)$ | 12.59 | 24.82 | 15.65 | 14.13 |
| $t_2(s)$ | 12.60 | 8.43 | 7.79 | 7.01 |
| $t_5(s)$ | 12.59 | 8.33 | 5.22 | 35.87 |

## IV. Simulation Results

The proposed approach for persistent monitoring has been extensively tested in simulations. In Fig. 5 we simulate $N = 25$ agents that have to persistently monitor a given path of interest $\mathcal{P} = \{\mathcal{P}_{12} \cup \mathcal{P}_{23} \cup \mathcal{P}_{34} \cup \mathcal{P}_{45} \cup \mathcal{P}_{56} \cup \mathcal{P}_{61}\}$, for the case of equal (Fig. 5-(a)) and different (Fig. 5-(b)) priority assignments. In this case, we designed $v = \sqrt{\dot{x}(\gamma)^2 + \dot{y}(\gamma)^2}$ to be constant, hence in a 1-clustered coverage condition, without priority assignments Fig. 5-(a), we have equal covering time and homogeneous monitoring frequency for all the points on the path. We depicted with colored squares (in red, green and blue) three points that belong to different parts of the path. In Table I we report the amount of the time spent by the agents in the proximity of each of these points, by considering a proximity radius of 0.5 m and by changing the priority factor $f_i$. The red point $w_1$ belongs to the subpath $\mathcal{P}_{12}$, i.e., $w_1 \in \mathcal{P}_{12}$, the green point $w_2 \in \mathcal{P}_{23}$, while the blue point $w_3 \in \mathcal{P}_{56}$. As we expect the amount of monitoring time is equal on the three points of interest when $f_1 = f_2 = f_5$ (Fig.5-(a)), while by considering $f_1 = 3f_2 = 3f_5$ it results that $t_1$ (the monitoring time for the point of interest $w_1$) is about three time as much as $t_2$ and $t_5$ (Fig.5-(b)). By selecting $f_2 = 1/2f_1$ and $f_5 = 1/3f_1$, it results that $t_1$ is twice $t_2$ and about three times as much as $t_5$. Finally by selecting $f_1 = 2f_2$ and $f_5 = 5f_2$, we have $t_2 \approx 1/2t_1$ and $t_2 \approx 1/5t_5$.

In Fig. 6 we show how the configuration $\tilde{\theta}^{\star(\lfloor N/2 \rfloor)} = \alpha\theta^{\star(\lfloor N/2 \rfloor)}$ changes with $\alpha$. In this simulative example we have $N = 15$ agents; in corrispondence of $\eta = \gcd(\alpha, N) > 1$ the configuration goes in clusters, i.e., for $\alpha = \{3, 5, 6\}$,

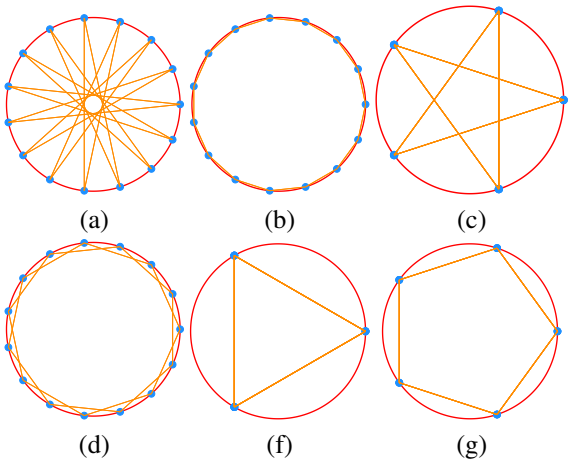


**Fig. 6:** Graphical representation of the equilibrium configuration at $\tilde{\theta}^{\star(\lfloor N/2 \rfloor)}$ multiplied by different values of $\alpha = \{1, 2, 3, 4, 5, 6\}$, by considering $N = 15$.

which are respectively Fig. 6-(c),(f),(g), while for $\alpha = \{1, 2, 4\}$, Fig. 6-(a),(b),(d), the system falls in 1-clustered coverage state configurations, since $\eta = 1$, in accordance with Lemma 2.

In Fig. 7 we depict an example for a three-dimensional mission space:

$$\mathcal{P}_{3D} : \begin{cases} x(\theta) = \sin(5\theta) \\ y(\theta) = \sin(\theta) \\ z(\theta) = \cos(3\theta) \end{cases} . \tag{5}$$

In this case we consider $N = 15$ agents, and we illustrate the final configurations for $\alpha = \{1, 3, 5, 15\}$ respectively from Fig. 7-(a) to 7-(d). Other paths with interesting properties in persistent monitoring and surveillance applications can be used in our framework, e.g., the Lissajous curves [3].

## V. Conclusions

We proposed a novel strategy for multi-robot persistent monitoring on closed paths. We used the idea of the time-inverted Kuramoto to achieve our goal. It permits to monitor a generic closed path in different configurations i.e., in splay-state configurations, and it allows to assign different priorities to the different locations on the path. Future works may consider the online path parametrization, hence dealing with time-varying paths. Other interesting directions may consider heterogeneous agents and the management of malicious attacks in the network. Finally, we plan to implement the algorithm on wheeled robots or UAVs.

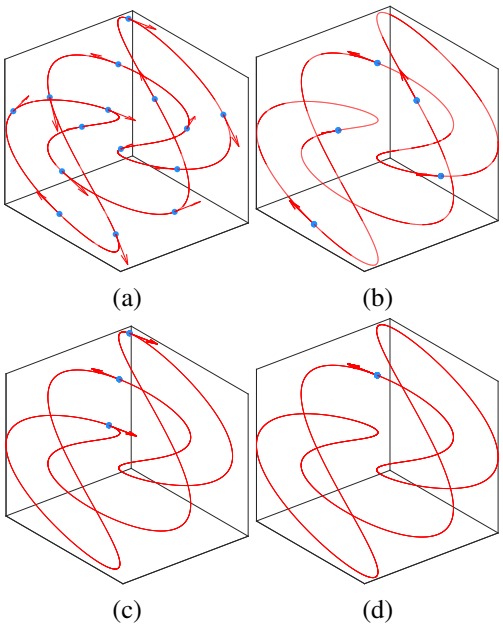


**Fig. 7:** Three dimensional persistent monitoring on the path $\mathcal{P}_{3D}$ in (5), by considering $N = 15$, $p = \lfloor N/2 \rfloor$ and $\tilde{\theta}_i = \alpha\theta_i$ with $\alpha = 2, 3, 5, 15$, respectively from (a) to (d).

## References


[1] Noa Agmon, Sarit Kraus, and Gal A Kaminka. Multi-robot perimeter patrol in adversarial settings. In *2008 IEEE International Conference on Robotics and Automation*, pages 2339–2345. IEEE, 2008.

[2] Manuel Boldrer, Francesco Riz, Fabio Pasqualetti, Luigi Palopoli, and Daniele Fontanelli. Time-inverted kuramoto dynamics for $\kappa$-clustered circle coverage. In *IEEE conference on decision and control (CDC)*. IEEE, 2021.

[3] Aseem Vivek Borkar, Arpita Sinha, Leena Vachhani, and Hemendra Arya. Application of lissajous curves in trajectory planning of multiple agents. *Autonomous Robots*, 44(2):233–250, 2020.

[4] Christos G Cassandras, Xuchao Lin, and Xuchu Ding. An optimal control approach to the multi-agent persistent monitoring problem. *IEEE Transactions on Automatic Control*, 58(4):947–961, 2012.

[5] Gene H Golub and Charles F Van Loan. *Matrix computations*. JHU press, 2013.

[6] Alexander Jahn, Reza Javanmard Alitappeh, David Saldaña, Luciano CA Pimenta, Andre G Santos, and Mario FM Campos. Distributed multi-robot coordination for dynamic perimeter surveillance in uncertain environments. In *2017 IEEE International Conference on Robotics and Automation (ICRA)*, pages 273–278. IEEE, 2017.

[7] Derek Kingston, Randal W Beard, and Ryan S Holt. Decentralized perimeter surveillance using a team of uavs. *IEEE Transactions on Robotics*, 24(6):1394–1404, 2008.

[8] Yoshiki Kuramoto. Self-entrainment of a population of coupled non-linear oscillators. In *International symposium on mathematical problems in theoretical physics*, pages 420–422. Springer, 1975.

[9] Joseph P La Salle. *The stability of dynamical systems*. SIAM, 1976.

[10] Xuchao Lin and Christos G Cassandras. An optimal control approach to the multi-agent persistent monitoring problem in two-dimensional spaces. *IEEE Transactions on Automatic Control*, 60(6):1659–1664, 2014.

[11] Fabio Pasqualetti, Joseph W Durham, and Francesco Bullo. Cooperative patrolling via weighted tours: Performance analysis and distributed algorithms. *IEEE Transactions on Robotics*, 28(5):1181–1188, 2012.

[12] Luciano CA Pimenta, Guilherme AS Pereira, Mateus M Gonçalves, Nathan Michael, Matthew Turpin, and Vijay Kumar. Decentralized controllers for perimeter surveillance with teams of aerial robots. *Advanced Robotics*, 27(9):697–709, 2013.

[13] David Saldana, Reza Javanmard Alitappeh, Luciano CA Pimenta, Renato Assunçao, and Mario FM Campos. Dynamic perimeter surveillance with a team of robots. In *International Conference on Robotics and Automation (ICRA)*, pages 5289–5294. IEEE, 2016.

[14] Stephen L Smith and Daniela Rus. Multi-robot monitoring in dynamic environments with guaranteed currency of observations. In *49th conference on decision and control (CDC)*, pages 514–521. IEEE, 2010.

[15] Stephen L Smith, Mac Schwager, and Daniela Rus. Persistent robotic tasks: Monitoring and sweeping in changing environments. *IEEE Transactions on Robotics*, 28(2):410–426, 2011.

[16] Daniel E Soltero, Stephen L Smith, and Daniela Rus. Collision avoidance for persistent monitoring in multi-robot systems with intersecting trajectories. In *2011 IEEE/RSJ International Conference on Intelligent Robots and Systems*, pages 3645–3652. IEEE, 2011.